

AN EXPERIMENTAL STUDY OF DROP MIGRATION IN SHEAR FLOW BETWEEN CONCENTRIC CYLINDERS

PAUL C.-H. CHAN† and L. G. LEAL

Department of Chemical Engineering, California Institute of Technology, Pasadena, CA 91125, U.S.A.

(Received 10 December 1979; in revised form 1 July 1980)

Abstract—The phenomenon of migration of liquid drops in Couette flow between concentric cylinders due to non-Newtonian fluid properties and shape deformation has been studied experimentally. The results agree very well with the theory of Chan and Leal, which included the effect of hydrodynamic interaction with the bounding walls, and that of velocity profile curvature in a Couette device. Significant observations that were not reported in previous studies include the migration of a deformable Newtonian drop to an equilibrium position between the centerline and the inner rotor, and the competition between normal stresses and shape deformation effects for the case of a Newtonian drop in a non-Newtonian fluid.

INTRODUCTION

Previous investigations conducted in our research group have examined the dynamics of particle migration in shearing flows. In our recent paper (Chan & Leal 1979) the roles of non-Newtonian rheology and shape deformation on the motion of a fluid drop were examined, based upon the assumptions of second-order fluid behavior, and weak deformation. It was found that the qualitative effects of these two mechanisms depend on the nature of the primary flow. For Poiseuille flow in a pipe, both contributions were predicted to produce particle motion towards the centerline. For planar Poiseuille flow, the qualitative effect of non-Newtonian fluid properties was predicted to remain the same, whereas that of drop deformation was found to depend on the value of the viscosity ratio between the two phases with the result that the drop might migrate either towards or away from the walls. For a Couette flow, the migration mechanism is even more complicated. In this case, both the non-Newtonian rheology and shape deformation effects are found to include two terms: one from hydrodynamic interaction between the particle and the walls, and a second due to the presence of velocity profile curvature in the Couette device. For non-Newtonian rheology alone, the net effect of these terms is predicted to be particle motion towards an equilibrium position between the centerline and the outer cylinder. On the other hand, the two contributions from drop deformation are predicted to result in an equilibrium position for the particle between the centerline and the inner rotor.

Although our theory for Poiseuille flow agrees very well with existing experimental observations (Goldsmith & Mason 1962, Gauthier *et al.* 1971a), the predictions for Couette flow have yet to be verified. In particular, the prediction that profile curvature will tend to cause a deforming Newtonian drop in a Newtonian suspending fluid to migrate inwards (i.e. towards the inner rotor) has not been demonstrated experimentally. In fact, inward migration in Couette flow has never even been predicted in any previous theory, regardless of the mechanism of migration that was considered, and has been observed in experiments only for rigid spheres in a "pseudoplastic" fluid. Since our prediction corresponds to drop motion towards the region of *largest* shape deformation, whereas all existing experimental observations show migration towards the region of *smallest* shape deformation, we feel that it is of fundamental interest to experimentally demonstrate the existence of inward migration for a deformable drop in a Couette flow.

In addition, our earlier theory also considered the effect of migration of a *spherical* drop due to non-Newtonian rheology of the suspending fluid or the drop, or both. It was concluded that the

†Present address: Dept. of Chemical Engineering, University of Rochester, Rochester, NY 14627, U.S.A.

drop would migrate in any of these cases to an equilibrium position between the outer cylinder and the centerline. The prediction that non-Newtonian rheology of the drop fluid alone would lead to particle migration is new. The predicted migration of a spherical Newtonian drop in a viscoelastic suspending fluid is also new, though the limiting case of a rigid spherical particle has been considered by several authors (Ho & Leal 1976; Brunn 1976a,b). However, in this limiting case, the theory is in apparent disagreement with existing experimental observations (Karnis & Mason 1966).

Finally, for situations which include both non-Newtonian rheology and drop shape deformation, our theory for a slightly non-Newtonian suspending fluid appears to be in qualitative agreement with the experiments by Gauthier *et al.* (1976b) who studied Newtonian drops in a viscoelastic suspending fluid. However, their experiments involved only one system of fluids, and in particular considered only large drop viscosities where the contribution of deformation to migration is always small compared to the non-Newtonian contribution. In addition, there have so far been *no* experiments on migration which involve non-Newtonian drops, and in spite of the fact that the contribution from non-Newtonian rheology is predicted to be numerically small in this case compared to that due to shape deformation, this is another area of interest for experimental study.

In the present paper, we report on experiments that were performed in our laboratory for the purpose of considering a number of these problem areas which have not previously been studied experimentally. The objective of these experiments was both to test the predictions of Chan and Leal under conditions where the theory should be applicable, and to determine the range of applicability of the theory by extension to the domains of stronger viscoelasticity and deformation. For each system of fluids, we varied the drop sizes and gap widths, as well as the shear rates. A general description of the experiments is given in the next section, followed by the results and discussions.

EXPERIMENTAL PART

(1) *Description of the apparatus*

The Couette device used in the experiments is illustrated in figure 1. It consisted of a 25-cm section of precision-bore glass cylinder (i.d. 12.0 cm) fitted onto an aluminum base and sealed with commercial silicone sealant RTV. A set of four solid aluminum cylinders (radii 1.27 cm, 2.54 cm, 3.81 cm, 4.60 cm respectively) were prepared as inner rotors. With one of these embedded in the aluminum base by means of a bearing, a plexiglass lid was fitted onto the top. By precisely matching each individual component, we were able to achieve accurate alignment of the apparatus while at the same time allowing it to be easily dismantled for maintenance or change of inner rotors. Only the inner cylinder was designed to rotate; this was accomplished by directly coupling it to a variable-speed motor and control system, as illustrated, which was capable of rotation at a constant speed (without fluctuations) at very low rates of revolution.

To set up the experiment, a 1-cm layer of mercury was poured onto the bottom of the tank, which was then filled with the suspending fluid, leaving only a small air gap between the top of the fluid and the lid on the concentric cylinder apparatus. The mercury acted as a nearly inviscid layer and was used in order to avoid secondary flows and to minimize any axial variations in the primary flow. The drops were injected through a slit in the top of the apparatus using a 10-cm long hypodermic needle (17 gauge) that was fed from a precision micrometer syringe. The drop sizes in our experiments varied from 5 to 50 μl . It was important that the drop sizes be measured accurately, since the migration velocity varies approximately linearly with the volume of the drop. The micrometer syringe which we used was accurate to 0.1 μl . However, an additional source of error was due to fluid loss when the tip of the syringe was actually pulled away from the drop. By direct observation of the radius of the residual droplets compared to that of the main drop, we estimated that the resulting uncertainty in the drop volume was always less than 5 per cent.

At the end of each experiment, the fluid drop was allowed to settle to the bottom of the

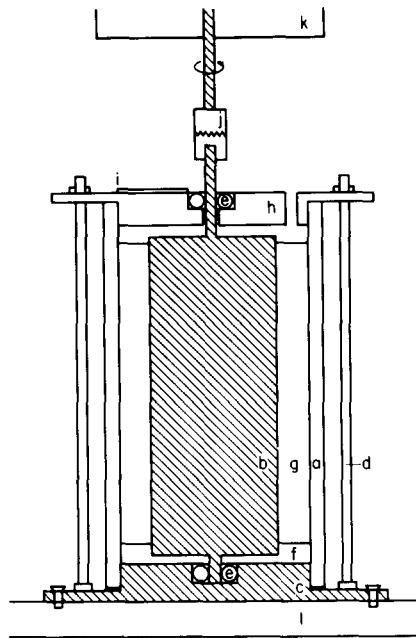


Figure 1. Schematic view of Couette flow device. a: precision bore glass cylinder; b: aluminum rotor; c: aluminum base; d: brass supporting rods; e: bearing; f: mercury layer; g: suspending fluid; h: plexiglass lid; i: scale; j: coupling; k: variable speed motor; l: wood panel.

apparatus (or rise to the top if it was lighter than the suspending fluid), where it would not affect other runs. Although we had attempted to find fluid systems with closely matched densities, a small density difference (not larger than $1/200 \text{ gm cm}^{-3}$) almost always existed, and hence the drop was often found to settle (or rise) out of the test region within approx. 3 hr.† In those few situations where the densities were “identical”, the drops had to be removed manually by suction using a large syringe. Thus, in all cases, the suspending fluid could be reused a number of times before it was replaced.

It should be noted that our apparatus was designed, for simplicity, without a constant temperature bath. However, the fluctuations in temperature are always small in our laboratory. In addition, viscous dissipation was clearly negligible at the low shear rates used in our experiments. Thus, the lack of a temperature control device in our apparatus is not believed to significantly affect the measured results.

Observation of the position of the drop during the experiment was achieved using a mirror inclined at 45° and positioned directly above the gap between the concentric cylinders. The plane of the mirror was parallel to a radial axis of the Couette device. Measurements were made by looking horizontally into the mirror using a cathetometer as a telescopic device. The cathetometer was mounted on a platform which could be moved in the radial direction, and thus we could observe the migration of the drop by adjusting the position of the cathetometer each time the drop came into view. The position of its center was then measured using a linear scale placed directly on the plexiglass top of the apparatus. The margin of error for this method was approx. 0.02 cm. For comparison, we note that the drop usually travelled a radial distance of no less than 0.5 cm in the course of a typical run.

(2) Materials

Previous experiments by Mason *et al.* (Goldsmith & Mason 1962; Gauthier *et al.* 1971a; Karnis & Mason 1966; Gauthier *et al.* 1971b; Karnis & Mason 1967) on the migration of

†It may be noted, however, that these small density differences are not significant insofar as the migration phenomenon is concerned, and the fluid drop can still be considered as neutrally buoyant for the purpose of comparing experimental results for migration with theoretical predictions. Obviously, this observation is correct only if the sedimentation velocity is small compared to the characteristic velocity, Ga , of the primary flow, as was always the case in our experiments.

Table 1.

Suspending phase		Suspended phase	σ (dyne cm^{-1})
1	Newtonian: Ucon oil LB-1715 ($\mu_0 = 9.0p$)	Water ($\bar{\mu}_0 = 0.01p$)	2.3
2		1 Per cent Separan AP-30 ($\bar{\mu}_0 = 24.8p$; batch a)	6.0
3		0.1 Per cent carboxyvinyl polymer in water ($\bar{\mu}_0 = 6.1p$)	5.1
4	Non-Newtonian: 1 per cent Separan AP-30 $\mu_0 = \begin{cases} 24.8p & \text{(batch a)} \\ 30.0p & \text{(batch b)} \\ 42.5p & \text{(batch c)} \end{cases}$	Silicone oil 510 fluid ($\bar{\mu}_0 = 1.1p$)	6.6
5		Ucon oil LB-1715 ($\bar{\mu}_0 = 9.0p$)	4.9

deformable drops were performed using various systems of drop and suspending fluids. In our case, however, the selection of fluids was considerably more difficult because the drops used in our experiments were generally larger (as we shall see in the following subsection, this was necessary to compensate for the wider gaps between the concentric cylinders when the smaller of the inner rotors was employed), and hence the densities of the fluids had to be more closely matched to minimize the velocity of drop sedimentation. As shown in table 1, each system consisted of an aqueous phase and an immiscible oil phase. It should be noted that we used Ucon oil LB-1715 throughout as our Newtonian suspending fluid because of its desirable physical properties and easy availability. Separan AP-30 (polyacrylamide manufactured by Dow Chemical C.) dissolved in water was chosen as the non-Newtonian suspending fluid in order to facilitate comparisons with the previous results by Gauthier, Goldsmith and Mason (1971b), who used Cyanamer P-250 (another brand of PAA).

To compare our experimental observations with theoretical predictions, it was necessary to estimate the interfacial tension and fluid viscosities for each system listed in table 1. The interfacial tension was obtained by determining the shape of the drop for one run at low shear rates, and calculating the interfacial tension using the formula for drop shape due to Taylor (1932). For this purpose, a camera was used to record the experiment on videotape, after which the lengths of the drop's major and minor axes were measured. The velocity gradient in the Couette device at the radial position of the drop center, R_0 , was calculated from the formula

$$\frac{\Omega_1 R_1^2}{R_2^2 - R_1^2} \left(1 + \frac{R_2^2}{R_0^2} \right)$$

for a device with appreciable curvature.† Although this procedure was somewhat inaccurate, as we shall discuss in more detail below, the fluid systems used in our experiments all had closely matched densities, and thus "conventional" methods of measuring interfacial tension could not be applied directly. In particular, both the pendant drop and spinning drop methods involve expressions for the interfacial tension which are linear in the density difference between the two fluids, and will therefore not give accurate results if the density difference is extremely small. The du Nouy ring method cannot be used for the simple reason that a "good" interface cannot often be formed between two fluids with nearly equal densities. In these cases, the interfacial tension must be obtained by the tedious procedure of extrapolating from measurements on fluids with nonzero density differences, as shown, for example, by the recent work of Kovitz & Yannimaras (1979). In contrast, the calculation of interfacial tension from a measured drop shape is obviously much simpler. However, the procedure is, at best, an approximate technique since Taylor's theory assumed linear shear flow and Newtonian rheology, whereas

†For the remainder of this paper, we adopt the same notation as used in Chan & Leal (1979).

profile curvature and non-Newtonian fluid properties were both present in our experiments to determine interfacial tension. As a partial justification of its use here, it may be noted that Taylor's expression suffices as a *valid first approximation* for a drop shape, provided that the particle size-to-gap width ratio is small, and the viscoelastic effect is *weak* (Chan & Leal 1979). Both conditions were satisfied in the experiments which were used to determine the interfacial tension, and the value of the deformation parameter $\delta \equiv a\mu_0 G/\sigma$ was always less than 0.2. In addition, it was shown by Gauthier, Goldsmith & Mason (1971b) that the discrepancy between theory and experiment for the deformation of a slightly non-Newtonian drop (1.5 per cent polyacrylamide in water) in a linear shear flow was only approx. 10 per cent for values of the deformation parameter δ up to 0.2, in qualitative agreement with our predictions. Finally, the results obtained here for systems 3 and 5 are consistent with the values obtained independently in our laboratory using the du Nouy tensiometer for a similar system of 1 per cent Separan AP-30 and Ucon oil LB-135 ($\sigma = 5$ dyne cm^{-1}), which has a nonzero density difference (Olbricht & Leal 1979). Thus, although it is difficult to quantify the accuracy of interfacial tension values listed in table 1, we believe that they are always within at least 15 per cent of the exact value.

The viscosity of each fluid was measured using a Cannon–Fenske viscometer. This device is clearly adequate for Newtonian materials; on the other hand, for fluids with shear-dependent viscosities, there may be some doubt as to the correct interpretation of the measurements. We estimate that the shear rate that applies for a typical Cannon–Fenske viscometer is always less than 0.1 s^{-1} , and hence most measured values may be taken as the viscosities of the fluids in the limit of zero shear.

The theory of Chan & Leal (1979) assumed that the viscoelastic fluids could be modelled as second-order fluids. In our case, there are no reported measurements in the literature on the rheological properties of aqueous Carbopol to test the applicability of this assumption. However, for 1 per cent Separan AP-30, it appears (Gauthier *et al.* 1971b, Leal *et al.* 1971, Blanks *et al.* 1974) that the viscosity actually reaches a constant value at a shear rate of 1 s^{-1} or less, which was always satisfied in our experiments. In addition, rod climbing experiments performed by Beavers & Joseph (1975) for 1.5 per cent Cyanamer P-250 in a glycerine–water mixture were well correlated by their second-order fluid theory for rotation rates of less than 10 s^{-1} . Thus, it appears that 1 per cent Separan AP-30 should behave as a second-order fluid under the conditions of our experiments. However, as we shall show later, this assumption appears to break down in the vicinity of the walls.

The zero-shear viscosities of Separan AP-30 solutions measured in this study (listed in table 1) were lower than those published by Leal *et al.* (1971) and by Blanks *et al.* (1974), but “agreed” with those of Gauthier, Goldsmith & Mason (1971b). In addition all three batches of solutions that were used had different viscosities, depending on the degree of agitation during mixing. However, it is well known that the rheological parameters of polymer solutions may change if the modes of preparation are different. Thus, the observed variations are not surprising, and the material properties of all three batches of Separan AP-30 in our experiments are qualitatively consistent with one another.

(3) *Conditions of the experiments*

One of the objectives of our present investigation was to observe the qualitative effect of velocity profile curvature on the migration of a fluid drop in Couette flow. Thus, for each system listed in table 1, we performed migration experiments using several different inner cylinders. When the largest rotor ($R_1 = 4.60$ cm) was used, the fluid's motion in the Couette apparatus could be approximated as a linear shear flow, i.e. the effect of profile curvature, though nonzero, was small. With decreasing rotor size, curvature became increasingly important. In fact, when the smallest rotor ($R_1 = 1.27$ cm) was used, the shear rate varied by a factor of ten across the gap, with the result that a drop which was nearly spherical when

released near the outer wall would be increasingly deformed if its migration was toward the inner wall. Indeed, with too high rotor speeds, and an inward direction of migration, some drops even broke up before reaching their equilibrium position. We did not measure the value of the deformation parameter δ at which breakup occurred for each different system listed in table 1, but for the case of a non-Newtonian drop in a Newtonian suspending fluid, it was estimated that the critical value of δ was approx. 0.6. This agrees with the observations of Gauthier, Goldsmith & Mason (1971b) for a moderate viscosity ratio $\kappa (= (\bar{\mu}_0/\mu_0))$, but it is generally agreed that the critical value will be much higher if κ is quite large or quite small. For our systems, when breakup occurred, the drops usually deformed into long threads which extended around the inner rotor, and then separated into smaller droplets when the apparatus was stopped.

In the theory of Chan & Leal (1979), both the deformation parameter δ and the non-Newtonian parameters λ and $\bar{\lambda}$ were assumed to be much less than unity. For each particular experiment, we could calculate directly the value of δ . However, we did not measure the normal stress coefficient ϕ_3 ; rather, λ (or $\bar{\lambda}$) was estimated by comparing the equilibrium positions predicted with those actually obtained (see Section 2 in Results and Discussion). In practice, the inferred magnitudes of λ (or $\bar{\lambda}$) were often of order unity, though the corresponding theory is only valid for $\lambda \ll 1$. One main reason for relaxing the conditions of small δ , λ and $\bar{\lambda}$ in the experiments was that they had to be carried out in a finite period of time, before secondary effects (e.g. drop sedimentation, partial solubility between the two fluid phases) became important. In addition, it was desired to test the usefulness of our theory beyond the asymptotic regime of $\delta \rightarrow 0$, $\lambda \rightarrow 0$, $\bar{\lambda} \rightarrow 0$ for which it is strictly valid. The values of δ , λ and $\bar{\lambda}$ evaluated at the centerline of the Couette device for each experiment are listed in the captions to the figures.

In addition to δ and λ , the size of the drop must also be small relative to the width of the gap in order for the theory to be applicable. Using the micrometer syringe, it was not possible to inject drops that were smaller than $5 \mu\text{l}$ in volume. Thus, the drop radius was always larger than 0.1 cm. When the largest rotor was used, the drop size to gap width ratio was approx. 0.1. For a larger gap, the size of the drops, as well as the angular velocity of the rotor, was also increased so that the migration velocity would remain finite, though in no case did the drop radius-to-gap width ratio ever exceed 0.1.

It is clear that flow instabilities (e.g. Taylor vortices) must not be allowed to occur in the Couette apparatus. For systems 1–3 in table 1 where the suspending fluid was Newtonian (Ucon oil), the maximum Taylor number was approx. 30, well below the established critical value of 3390. When the suspending fluid was Seqaran AP-30, the effect of viscoelasticity on stability must be considered. In these experiments, inertial effects were negligible compared to non-Newtonian fluid rheology, and the relevant stability analysis is that of Giesekus (1966) for a viscoelastic fluid. Since the non-Newtonian parameter λ was always below its predicted critical value of approx. 3.5, no instability should be expected and, indeed, no evidence of an instability was observed.

RESULTS AND DISCUSSION

(1) A Newtonian drop in a Newtonian fluid

Previous experiments on the migration of a Newtonian drop suspended in a Couette flow of a Newtonian fluid were reported by Karnis & Mason (1967) for water drops in silicone oil. For a narrow gap, the drop was observed to migrate to an equilibrium position which was very close to the centerline of the Couette device. However, no equilibrium positions were reported for larger gap widths. Since the theory of Chan & Leal (1979) predicts that profile curvature is an important factor in determining the equilibrium position of a drop in Couette flow, we have repeated the Karnis and Mason experiments using water drops suspended in Ucon oil LB-1715 (which had the advantage over the previous systems that the densities were more closely

matched) in order to study carefully the effect of profile curvature by systematically altering the size of the inner rotor, while holding the size of the outer cylinder fixed.

In all cases, the drops were observed to migrate towards an equilibrium position which was between the centerline and the inner cylinder. Furthermore, the equilibrium position was near the centerline only for the case of a "narrow gap" Couette device. As the profile curvature increased, the equilibrium position moved closer to the inner cylinder. These observations are in qualitative agreement with the predictions of our theory. In figure 2, we plot the experimentally measured and theoretically predicted trajectories of the drops for each rotor size. The solid lines were obtained by summing the wall reflexion and profile curvature contributions, and then integrating to give ([8.4] and [8.5] of Chan & Leal 1979),

$$T = \frac{d\sigma}{\mu_0} \int_{s_0}^s \frac{ds}{Z(s)} \quad [1]$$

where

$$Z(s) = \frac{\Omega_1^2 R_1^4 R_2^4}{(R_2^2 - R_1^2)^2} \left\{ \frac{a^4}{d^2} \left(\frac{1}{R_0^2} + \frac{1}{R_2^2} \right)^2 \frac{3(16 + 19\kappa)(54 + 97\kappa + 54\kappa^2)}{4480(1 + \kappa)^3} \right. \\ \left. \times \left[\frac{1}{s^2} - \frac{1}{(1-s)^2} + 2(1-2s) \right] - \frac{2(4 + 61\kappa + 85\kappa^2 + 25\kappa^3)}{7(2 + 3\kappa)(1 + \kappa)^2} \frac{a^3}{R_0^3} \right\}. \quad [2]$$

The material parameters σ , μ_0 , κ were already listed in table 1, whereas a , R_1 , R_2 , R_0 , d were all measurable for any particular Couette flow geometry. Thus, for each migration experiment, we could predict the trajectory of the drop after numerically integrating [1]. Under ideal conditions (asymptotically small drop deformation and velocity profile curvature) when our theory is expected to be valid, the accuracy of the prediction depends mainly on the accuracies to which the interfacial tension σ and the drop volume can be measured. Thus, for each predicted trajectory, the value of T as a function of position is accurate to within 20 per cent. In addition, the actual measurement of (dimensionless) drop position s may have an error of ± 0.02 .

We have plotted the measured and predicted trajectory for each migration experiment in figures 2(a)–2(d). The corresponding value of the deformation parameter, δ , is listed in the captions. For cases 2(a) and 2(b) where the gap of the Couette device is small, the agreement between theory and experiment is extremely good, even though δ is as large as 0.684. We conclude, from this, that our deformation theory for a quadratic shear flow between two parallel *plane* walls is valid at least up to $\delta \sim 0.7$. On the other hand, when smaller inner rotors were used (cases 2(c) and 2(d)), the theory begins to break down, as expected, even for smaller values of δ . Clearly, in these cases, the wall reflexions procedure for two parallel *plane* walls is no longer valid, in spite of the fact that the qualitative agreement between theory and experiment is still quite good. Furthermore, it should be noted that the predicted inward migration rate for these cases is always smaller than the experimentally measured values. This discrepancy may be attributed in part to the fact that the contribution to migration from hydrodynamic interaction with the inner rotor is overestimated when the radius of the inner rotor is small, since our calculation is based on two parallel plane walls. In addition, it seems likely that the effect of the outer cylinder will actually be larger than that predicted for a plane wall located at the same distance.

(2) A viscoelastic drop in a Newtonian fluid

There have been no previous experiments on the migration of a viscoelastic drop suspended in Couette flow of a Newtonian fluid. For the present investigation, we chose two aqueous polymer solution as drops and Ucon oil LB-1715 as the suspending phase (systems 2 and 3 in

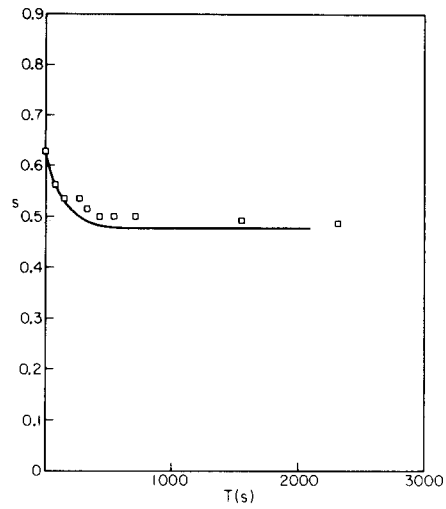


Figure 2(a).

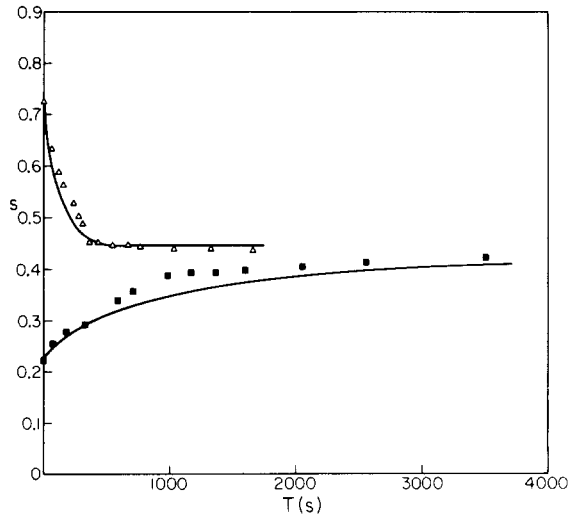


Figure 2(b).

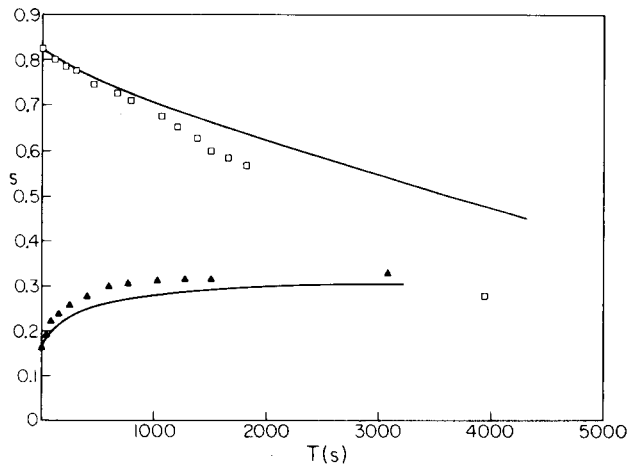


Figure 2(c).

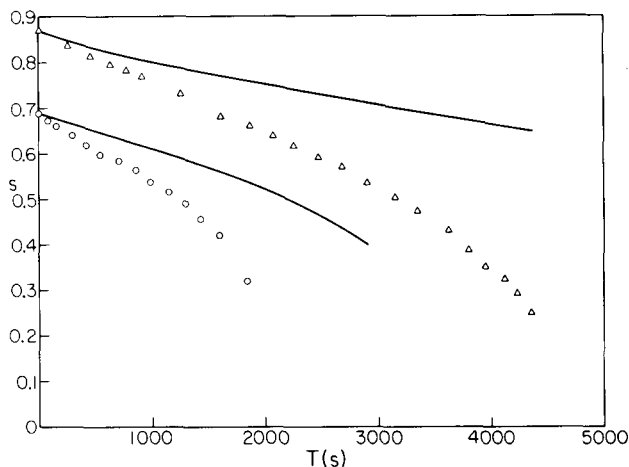


Figure 2(d).

Figure 2. A comparison of experimental trajectory with theory (—) for system 1. (a) $R_1 = 4.60$ cm, \square , $a = 0.134$ cm, $\Omega_1 = 0.269$ s $^{-1}$, $\delta = 0.459$. (b) $R_1 = 3.81$ cm, \blacksquare , $a = 0.134$ cm, $\Omega_1 = 0.269$ s $^{-1}$, $\delta = 0.238$; Δ , $a = 0.193$ cm, $\Omega_1 = 0.537$ s $^{-1}$, $\delta = 0.684$. (c) $R_1 = 2.54$ cm, \square , $a = 0.134$ cm, $\Omega_1 = 1.05$ s $^{-1}$, $\delta = 0.358$; \blacktriangle , $a = 0.193$ cm, $\Omega_1 = 0.537$ s $^{-1}$, $\delta = 0.263$. (d) $R_1 = 1.27$ cm, Δ , $a = 0.193$ cm, $\Omega_1 = 2.11$ s $^{-1}$, $\delta = 0.278$; \circ , $a = 0.229$ cm, $\Omega_1 = 2.11$ s $^{-1}$, $\delta = 0.330$.

table 1). The migration effects for these systems were expected to result from a combination of drop deformation and non-Newtonian rheology.

Qualitatively, it was found that there were no changes in the behavior of the drops from the previous Newtonian case where the only migration mechanism is shape deformation, i.e. they migrated to an equilibrium position which was between the centerline and the inner cylinder. However, by comparing the experimentally measured equilibrium positions with those predicted by the Newtonian deformation theory, it is evident that the non-Newtonian properties of the drop fluid were playing a nontrivial role in the migration process. The predicted magnitude of this contribution for a second-order fluid is given by [5.10] and [5.20] of Chan & Leal (1979). If we sum the separate deformation and non-Newtonian terms (letting $\bar{\epsilon}_1 \approx -\mathcal{E}.60$; our results are not sensitive to the exact magnitude of $\bar{\epsilon}_1$, as long as it is within the generally accepted range of -0.5 – -0.6 as discussed in Leal 1975), and integrate, we again obtain [1], where in this case

$$\begin{aligned}
 Z(s) = & \frac{\Omega_1^2 R_1^4 R_2^4}{(R_2^2 - R_1^2)^2} \left\{ \frac{a^4}{d^2} \left(\frac{1}{R_0^2} + \frac{1}{R_2^2} \right)^2 \frac{3}{4480(1+\kappa)^3} \left[(16 + 19\kappa)(54 + 97\kappa + 54\kappa^2) \right. \right. \\
 & + 8(33.8 + 63\kappa) \frac{\bar{\phi}_3 \sigma}{a\mu_0^2} \left. \left. \left[\frac{1}{s^2} - \frac{1}{(1-s)^2} + 2(1-2s) \right] - \frac{2}{21(2+3\kappa)(1+\kappa)^2} \right. \right. \\
 & \left. \left. \times \left[3(4 + 61\kappa + 85\kappa^2 + 25\kappa^3) - 8.8 \frac{\bar{\phi}_3 \sigma}{a\mu_0^2} \right] \frac{a^3}{R_0^3} \right\}. \quad [3]
 \end{aligned}$$

In the above expression, the first term is due to the presence of the bounding walls, and will always contribute to migration towards the center of the Couette device. The second term comes from profile curvature, and has two contributions which tend to oppose each other, with the net effect depending on the parameter $(\bar{\phi}_3 \sigma / a\mu_0^2) (= (\kappa \bar{\lambda} / \delta))$, which measures the relative importance of deformation and non-Newtonian effects. Under “normal” conditions, it can be shown that the deformation term will always dominate *numerically*. Thus, despite the fact that the parameter $\bar{\phi}_3 \sigma / a\mu_0^2$ itself was quite large in our experiments (see values of δ and $\bar{\lambda}$ in figures 3 and 4), the equilibrium position is again predicted to be between the centerline and the inner cylinder, in agreement with the experimental observations.

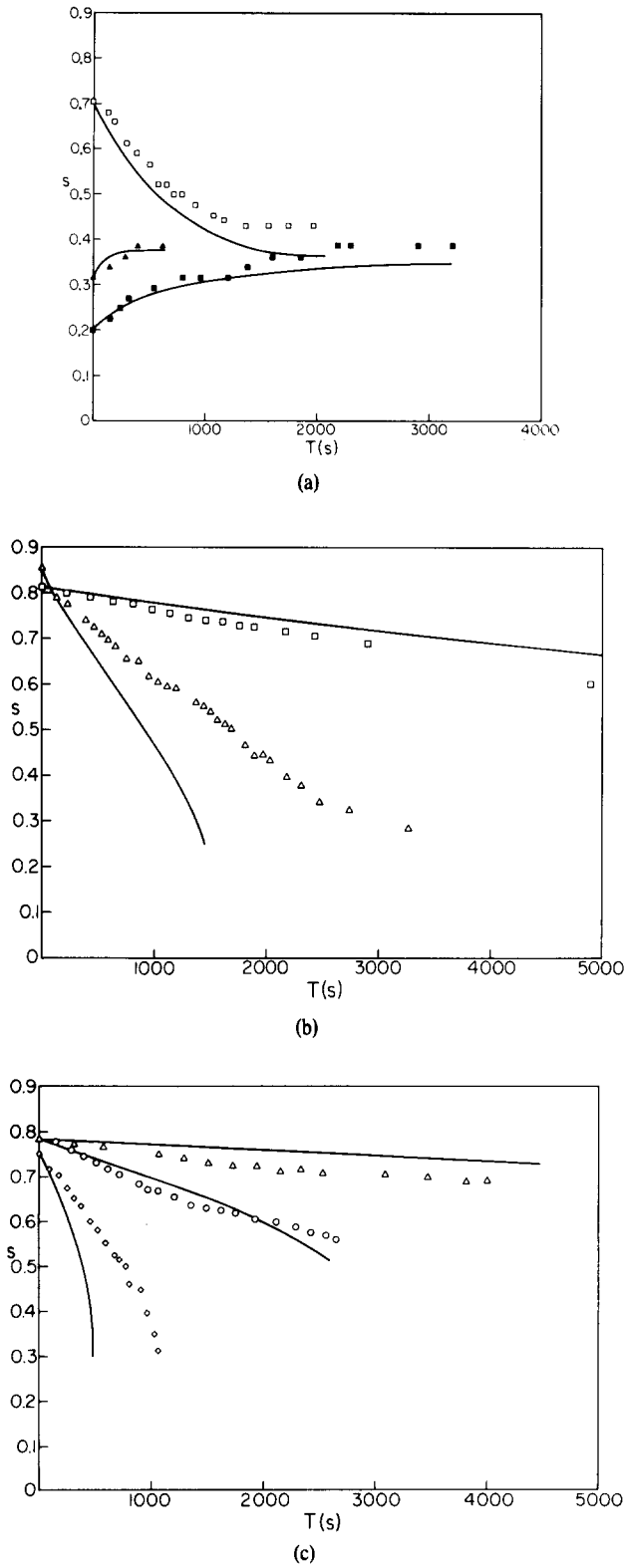


Figure 3. A comparison of experimental trajectory with theory (—) for system 2 (assuming $\bar{\phi}_3 = 54$ dyne s 2 cm $^{-2}$). (a) $R_1 = 3.81$ cm. \square , $a = 0.134$ cm, $\Omega_1 = 0.537$ s $^{-1}$, $\delta = 0.182$, $\lambda = 1.97$; \blacksquare , $a = 0.134$ cm, $\Omega_1 = 0.269$ s $^{-1}$, $\delta = 0.091$, $\lambda = 0.98$; \blacktriangle , $a = 0.193$ cm, $\Omega_1 = 0.537$ s $^{-1}$, $\delta = 0.262$, $\lambda = 1.97$. (b) $R_1 = 2.54$ cm. \square , $a = 0.134$ cm, $\Omega_1 = 0.537$ s $^{-1}$, $\delta = 0.070$, $\lambda = 0.759$; \triangle , $a = 0.193$ cm, $\Omega_1 = 1.05$ s $^{-1}$, $\delta = 0.197$, $\lambda = 1.49$. (c) $R_1 = 1.27$ cm. \triangle , $a = 0.193$ cm, $\Omega_1 = 1.05$ s $^{-1}$, $\delta = 0.053$, $\lambda = 0.399$; \circ , $a = 0.229$ cm, $\Omega_1 = 2.11$ s $^{-1}$, $\delta = 0.127$, $\lambda = 0.803$; \diamond , $a = 0.229$ cm, $\Omega_1 = 5.11$ s $^{-1}$, $\delta = 0.307$, $\lambda = 1.94$.

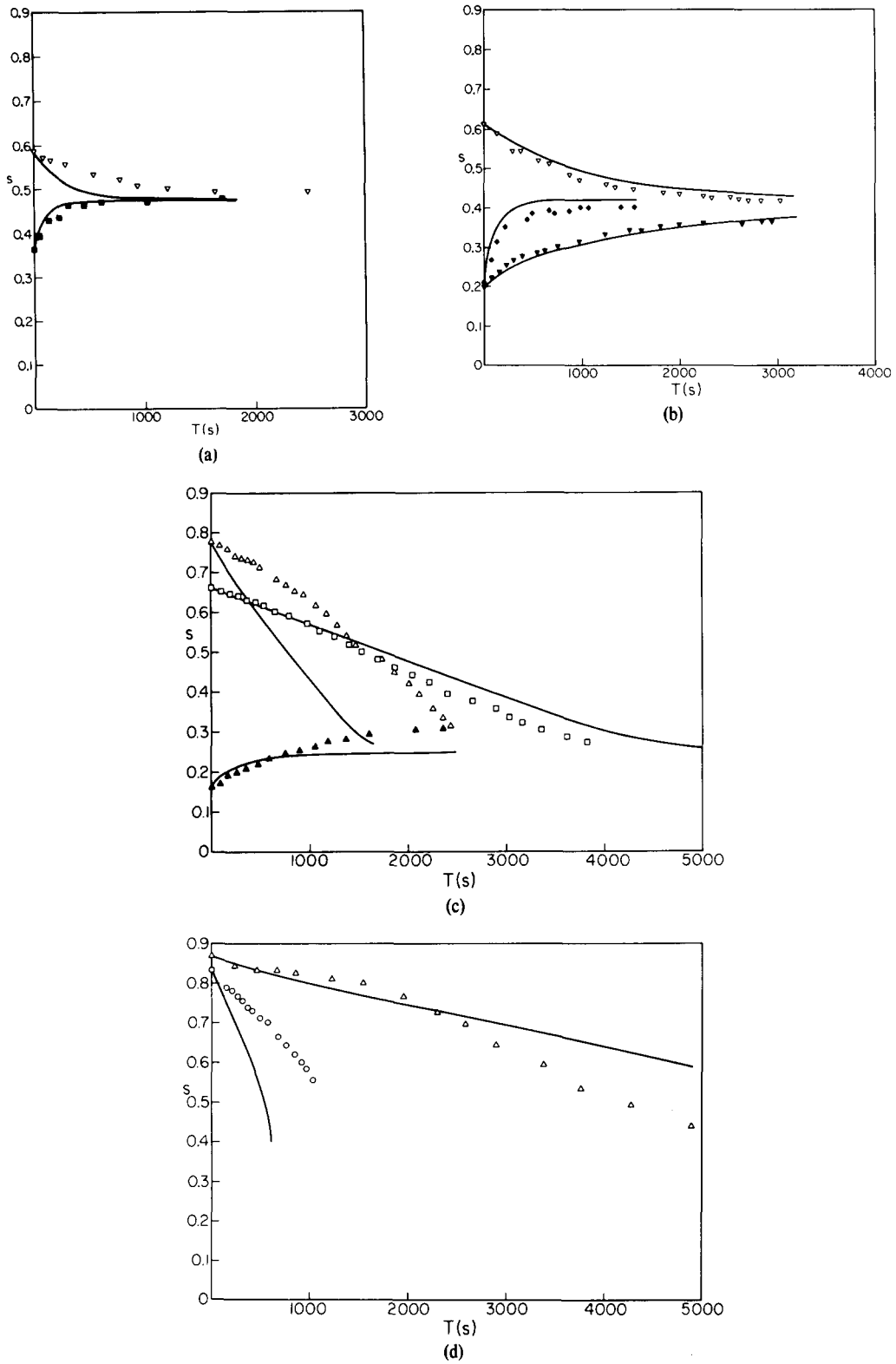


Figure 4. A comparison of experimental trajectory with theory (—) for system 3 (assuming $\bar{\phi}_3 = 22 \text{ dyne s}^2 \text{ cm}^{-2}$). (a) $R_1 = 4.6 \text{ cm}$, ∇ , $a = 0.106 \text{ cm}$, $\Omega_1 = 0.269 \text{ s}^{-1}$, $\delta = 0.164$, $\bar{\lambda} = 3.16$; \blacksquare , $a = 0.134 \text{ cm}$, $\Omega_1 = 0.269 \text{ s}^{-1}$, $\delta = 0.207$, $\bar{\lambda} = 3.16$. (b) $R_1 = 3.81 \text{ cm}$, \blacktriangledown , $a = 0.106 \text{ cm}$, $\Omega_1 = 0.269 \text{ s}^{-1}$, $\delta = 0.085$, $\bar{\lambda} = 1.64$; ∇ , $a = 0.106 \text{ cm}$, $\Omega_1 = 0.537 \text{ s}^{-1}$, $\delta = 0.169$, $\bar{\lambda} = 3.27$; \blacklozenge , $a = 0.161 \text{ cm}$, $\Omega_1 = 0.537 \text{ s}^{-1}$, $\delta = 0.257$, $\bar{\lambda} = 3.27$. (c) $R_1 = 2.54 \text{ cm}$, \square , $a = 0.134 \text{ cm}$, $\Omega_1 = 1.05 \text{ s}^{-1}$, $\delta = 0.161$, $\bar{\lambda} = 2.46$; \blacktriangle , $a = 0.193 \text{ cm}$, $\Omega_1 = 0.537 \text{ s}^{-1}$, $\delta = 0.119$, $\bar{\lambda} = 1.26$; \triangle , $a = 0.193 \text{ cm}$, $\Omega_1 = 1.05 \text{ s}^{-1}$, $\delta = 0.232$, $\bar{\lambda} = 2.46$. (d) $R_1 = 1.27 \text{ cm}$, \triangle , $a = 0.193 \text{ cm}$, $\Omega_1 = 2.11 \text{ s}^{-1}$, $\delta = 0.126$, $\bar{\lambda} = 1.33$; \circ , $a = 0.229 \text{ cm}$, $\Omega_1 = 5.11 \text{ s}^{-1}$, $\delta = 0.361$, $\bar{\lambda} = 3.22$.

In order to predict the detailed trajectory of the drop, we still need a quantitative estimate for the parameter $\tilde{\phi}_3\sigma/\mu_0^2$. This may be accomplished by measuring $\tilde{\phi}_3$ directly for any particular non-Newtonian fluid that is used (e.g. using a Weissenberg rheogoniometer or by means of rod climbing experiments). However, an alternate method which we have used here is to observe that the function $Z(s)$ is zero when the drop is at its equilibrium position, so that $\tilde{\phi}_3$ may be estimated indirectly from [3], all other variables being measurable experimentally. Although this means that the predicted and measured equilibrium positions are forced to coincide, the theory is still subjected to two reasonably stringent tests by this procedure. First, the inferred values of $\tilde{\phi}_3$ can be compared with existing literature estimates obtained via normal stress or other measurements. Second, the measured trajectories can be compared with [1] and [3]. The fact that the final equilibrium position is forced to coincide does not insure that the rest of the trajectory will be correctly predicted unless the theory is, in fact, correct. For 1 per cent Separan AP-30 solution (batch a), we find that a value of $\tilde{\phi}_3$ equal to 54 dyne s² cm⁻² provides a good fit to the experimental data for the present case of a viscoelastic drop in a Newtonian fluid, as well as for the next case of a Newtonian drop in a viscoelastic fluid. This value is consistent with existing estimates of the normal stress coefficient of Separan, as we shall show in the next section. In addition, the fact that one value of $\tilde{\phi}_3$ can be used to match the trajectories of both sets of experiments is an extremely strong confirmation of the theory and of its applicability under conditions of the present experiments. The predicted trajectories for a Separan drop in Ucon oil, using $\tilde{\phi}_3 = 54$ dyne s² cm⁻², are compared with experimentally observed ones in figure 3. With the exception of two cases in 3(b) and 3(c), the fit between data and predictions is excellent. In the latter two cases, the experimentally measured inward migration rates were *smaller* than our theoretical predictions, in contrast to our observations in the Newtonian-Newtonian problems of the previous subsection. Hence, this discrepancy must clearly be attributed to non-Newtonian effects alone. In addition it should be noted that the disagreement between theory and experiment is large only when a wide gap Couette device is used, *and* when the shear rate (hence the value of $\bar{\lambda}$) is high. Since the wall reflection procedure in our theory depends critically on the assumption of two parallel plane walls, it may be hypothesized that the predicted wall contribution to the migration of a non-Newtonian drop in a wide gap Couette device is suspect (and, in fact, always *overestimates* the wall effect) when $\bar{\lambda}$ is larger than 1.5. This hypothesis will be discussed in more detail in the final section of this paper.

For 0.1 per cent Carbopol in water, the procedures outlined above yield an estimate for $\tilde{\phi}_3\sigma/\mu_0^2$ of 1.4 cm, in which case $\tilde{\phi}_3$ is approx. 22 dyne s² cm⁻². This is certainly a reasonable value of $\tilde{\phi}_3$ for a dilute polymer solution, although there are no previous experiments that we could locate on the rheological properties of Carbopol in water. The predicted trajectories with $\tilde{\phi}_3 = 22$ dyne s² cm⁻² are plotted together with the observed trajectories in figure 4. From the apparent consistency between theory and experiment, it appears that our second-order theory for drop migration is applicable, even though there are no definitive indications (from rheological measurements) that 0.1 per cent Carbopol in water should obey the second-order fluid model at the shear rates used in the experiments. Once again, the discrepancy between theory and experiment becomes larger when the shear rate and curvature are increased, which is consistent with our previous observations.

Table 2.

κ	$\left(\frac{\phi_3\sigma}{a\mu_0^2}\right)_{cr}$
0.01	0.80
0.1	1.30
1	2.02
10	1.66

(3) A Newtonian drop in a viscoelastic fluid

To supplement the previous work by Gauthier *et al.* (1971b) on drop migration in Couette flow of a non-Newtonian fluid, we have performed additional experiments using fluids of different viscosities and a systematic variation in the size of the inner rotor. The predicted trajectories of the drop are again obtained as before. In this case, for $\epsilon_1 \approx -0.6$, we have

$$Z(s) = \frac{\Omega_1^2 R_1^4 R_2^4}{(R_2^2 - R_1^2)^2} \left\{ \frac{a^4}{d^2} \left(\frac{1}{R_0^2} + \frac{1}{R_2^2} \right)^2 \frac{1}{4480(1 + \kappa)^3} \left[3(16 + 19\kappa)(54 + 97\kappa + 54\kappa^2) \right. \right. \\ \left. \left. + 2(324.8 + 1234.8\kappa + 1700.4\kappa^2 + 866\kappa^3) \frac{\phi_3 \sigma}{a\mu_0^2} \right] \left[\frac{1}{s^2} - \frac{1}{(1-s)^2} + 2(1-2s) \right] \right. \\ \left. - \frac{1}{63(2+3\kappa)(1+\kappa)^2} \left[18(4+61\kappa+85\kappa^2+25\kappa^3) \right. \right. \\ \left. \left. - (99.2+451.2\kappa+714.4\kappa^2+294\kappa^3) \frac{\phi_3 \sigma}{a\mu_0^2} \right] \frac{a^3}{R_0^3} \right\}. \quad [4]$$

In contrast to our conclusions in the previous two subsections where the contribution due to drop deformation is numerically dominant, in the present systems the effects of deformation and non-Newtonian rheology are comparable in magnitude, and hence the equilibrium position of the drop (whether it is closer to the inner or outer wall) will critically depend on the material properties of the fluids. In fact, for a given viscosity ratio κ , we may calculate a value of the parameter $\phi_3 \sigma / a\mu_0^2$ at which the second term in [4] changes sign, with the result that the equilibrium position of the drop moves from one side of the centerline to the other. These critical values for $\phi_3 \sigma / a\mu_0^2$ are listed as a function of κ in table 2.

Our experimental results were in fact in good agreement with the predicted trajectories. Indeed, by comparing the measured and predicted trajectories, we estimate that ϕ_3 is approx. 60 dyne s² cm⁻² for batch b of 1 per cent Separan AP-30 in water, and 68 dyne s² cm⁻² for batch c. These estimates, together with the value of 54 dyne s² cm⁻² for batch a, which is used here as well as in the last subsection, appear to be self-consistent since the intrinsic time scales of *all three* batches (i.e. ϕ_3 / μ_0) are then approx. 2 sec. Furthermore, they are also consistent with the measurements by Bartram *et al.* (1975) for 2.5 per cent PAA in water (see Leal 1975), and with the calculations by Chan & Leal (1979) for the 4 per cent solution. The experimental data and predicted trajectories for systems 4 and 5 are shown in figures 5 and 6.

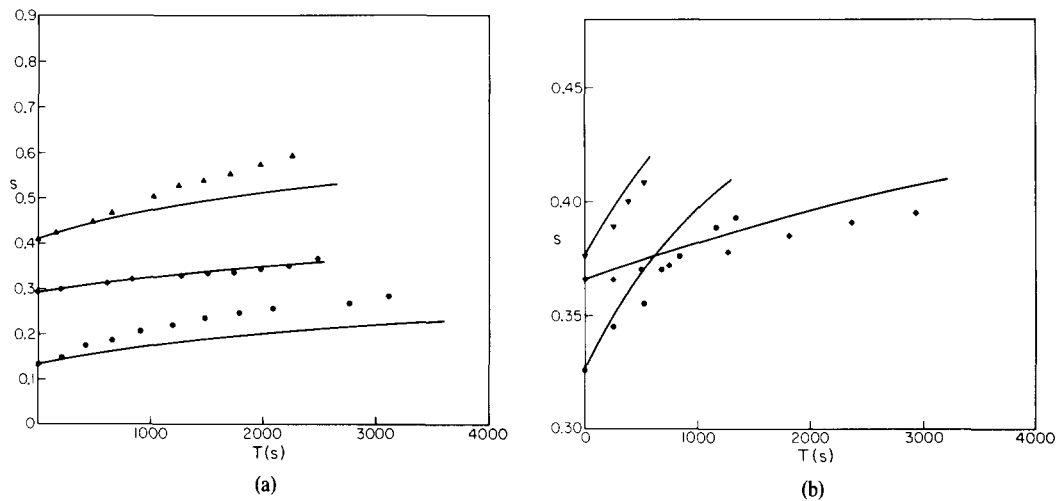
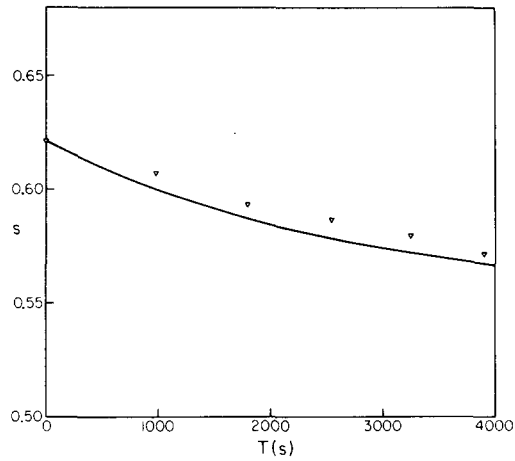
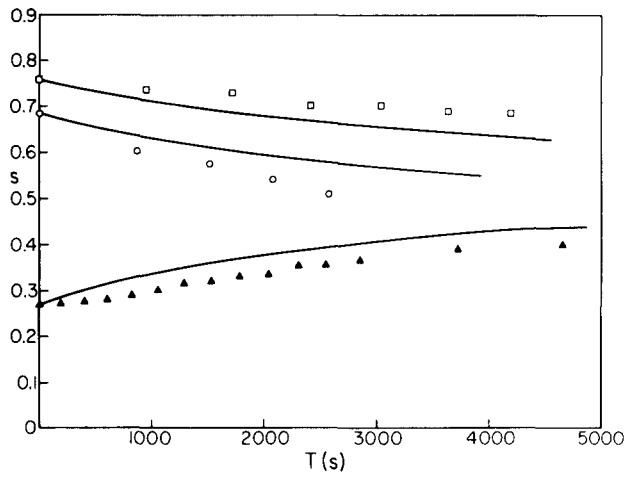


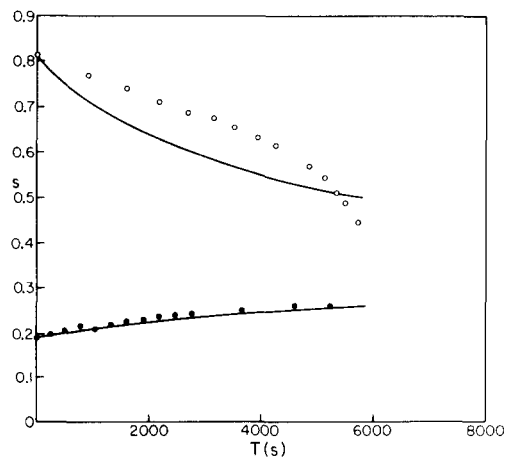
Figure 5. A comparison of experimental trajectory with theory (—) for system 4. (a) $R_1 = 2.54$ cm. Batch b ($\phi_3 = 60$ dyne s² cm⁻²). $a = 0.229$ cm, ●, $\Omega_1 = 0.0524$ s⁻¹, $\delta = 0.035$, $\lambda = 0.068$; ◆, $\Omega_1 = 0.105$ s⁻¹, $\delta = 0.071$, $\lambda = 0.136$; ▲, $\Omega_1 = 0.262$ s⁻¹, $\delta = 0.177$, $\lambda = 0.340$. (b) $R_1 = 1.27$ cm. Batch c ($\phi_3 = 68$ dyne s² cm⁻²). ▼, $a = 0.106$ cm, $\Omega_1 = 2.01$ s⁻¹, $\delta = 0.240$, $\lambda = 0.562$; ●, $a = 0.229$ cm, $\Omega_1 = 1.03$ s⁻¹, $\delta = 0.265$, $\lambda = 0.288$; ◆, $a = 0.229$ cm, $\Omega_1 = 0.524$ s⁻¹, $\delta = 0.135$, $\lambda = 0.147$.



(a)



(b)



(c)

Figure 6. A comparison of experimental trajectory with theory (—) for system 5. (a) $R_1 = 4.60$ cm. Batch a ($\phi_3 = 54$ dyne $\text{s}^2 \text{cm}^{-2}$). ∇ , $a = 0.106$ cm, $\Omega_1 = 0.0524$ s^{-1} , $\delta = 0.092$, $\lambda = 0.371$. (b) $R_1 = 3.81$ cm. Batch a. \square , $a = 0.134$ cm, $\Omega_1 = 0.105$ s^{-1} , $\delta = 0.120$, $\lambda = 0.386$; \blacktriangle , $a = 0.193$ cm, $\Omega_1 = 0.0524$ s^{-1} , $\delta = 0.086$, $\lambda = 0.192$; \circ , $a = 0.229$ cm, $\Omega_1 = 0.0524$ s^{-1} , $\delta = 0.102$, $\lambda = 0.192$. (c) $R_1 = 2.54$ cm. Batch b ($\phi_3 = 60$ dyne $\text{s}^2 \text{cm}^{-2}$). $a = 0.229$ cm, \bullet , $\Omega_1 = 0.0524$ s^{-1} , $\delta = 0.048$, $\lambda = 0.068$; \circ , $\Omega_1 = 0.262$ s^{-1} , $\delta = 0.239$, $\lambda = 0.340$.

It should be noted, for some situations in which a silicone oil drop (system 4) migrated outwards at the start of the experiment, that it would *reverse* its direction of motion after approximately half an hour. We attribute this occurrence to a change in the relative magnitudes of the deformation and non-Newtonian contributions, which is reflected in a *decrease* of the parameter $\phi_3\sigma/\mu_0^2$. Clearly, a change in the temperature within the Couette device could cause this phenomenon; however, viscous dissipation is negligible in the present experiments. A much more plausible explanation, based upon observations of the shape of the drop at different time intervals, is that the interfacial tension between Separan AP-30 and silicone oil 510 fluid is gradually decreasing during the experiments. Most probably, this change in interfacial tension is due to a very slight solubility of polyacrylamide molecules in the silicone oil. Since the relative magnitudes of the deformation and non-Newtonian rheology contributions to the migration velocity are closely competitive in the present situation, a slight decrease in the value of the interfacial tension could easily cause a "reversal" in the direction of migration. Estimates of the interfacial tension from photographs of the drop shape at the point of reversal indicated that the decrease in interfacial tension was as large as 20 per cent before reversal occurred. It may be noted that a much larger decrease (threefold) had been reported by Grace (1971) for another presumably immiscible system. In any case, we have omitted the portions of the trajectories where reversal occurred from figure 5.

It may appear at first that our results in this subsection are in qualitative disagreement with those of Gauthier *et al.* (1971b), who for a similar system always observed equilibrium positions which were between the centerline and the other cylinder, with no reversal in the direction of particle motion. However, we note that the radii of the drops in the previous experiments were smaller than ours by a factor of three, plus the viscosity of the suspending fluid (1.5 per cent PAA in water) was also considerably lower. In their case, then, the contribution due to drop shape deformation was clearly minimized, as evidenced by a larger value of $\phi_3\sigma/a\mu_0^2$. Thus, Mason's experiments were carried out in a regime where non-Newtonian rheology was dominant, so that the equilibrium position of the drop was between the centerline and the outer wall, as expected. Our experiments, on the other hand, included both non-Newtonian rheology and drop shape deformation effects of comparable magnitude (see the values of δ and λ listed in the captions to figures 5 and 6), and hence the equilibrium positions could be on either side of the centerline. This observation may perhaps be best illustrated by considering specifically figures 5(a) and 6(c), where the experimental conditions were identical except for the viscosity ratios $\bar{\mu}_0/\mu_0$ and the values of the parameter $\phi_3\sigma/a\mu_0^2$. For silicone oil 510 fluid ($\bar{\mu}_0 = 1.1\rho$), $\phi_3\sigma/a\mu_0^2$ equals 1.92, which is greater than its critical value of 0.98, and hence the equilibrium position is closer to the outer cylinder, as expected. The inverse was true for Ucon oil LB-1715. Thus, in spite of the fact that the observed equilibrium positions for our systems are different from Mason's, the results are not contradictory as might first appear to be the case. In fact, both Mason's results and the present results are qualitatively consistent with the predictions of Chan & Leal (1979). The case of dominant drop deformation was considered in the previous two subsections.

CONCLUDING COMMENTS

We have performed experiments on drop migration in Couette flow which have been compared with the theoretical predictions of Chan & Leal (1979). For the case of a deformable Newtonian drop in a Newtonian fluid, the equilibrium position was always between the centerline and the inner wall. If non-Newtonian rheology was then included, the equilibrium position moved outwards. The effect of velocity profile curvature was to determine quantitatively how this would occur, i.e. for larger profile curvature, the equilibrium position was further away from the centerline. Of course, the *rate* of migration depends on the numerical values of all the material parameters of the fluids in any system that is used.

In spite of the qualitative success of the drop migration theory, one important difficulty remains to be resolved, namely the fact that the wall contribution to non-Newtonian migration appears to be always overestimated. This discrepancy manifests itself most distinctly in the limiting case of migration of a *rigid* sphere in a viscoelastic fluid, where Karnis & Mason (1966) observed migration to the outer wall for a sphere in 4 per cent PAA in water, whereas our theory predicts an equilibrium position between the outer wall and the centerline. Recent experiments performed in our laboratory using polystyrene spheres and 1 per cent Separan AP-30 showed the same behavior as the earlier results of Karnis and Mason. Another apparent manifestation of the same difficulty is the apparent discrepancy between theory and experiment for the migration rates of drops when λ (or $\tilde{\lambda}$) is not vanishingly small, as we noted earlier in this paper. Indeed, careful examination of the results of Gauthier *et al.* (1971b) also shows the same problem. One plausible explanation of the apparent difficulty with the theory for estimating wall effects in a viscoelastic fluid is that the influence of viscoelasticity is greatly increased near the walls, so that the second-order fluid expansion may not be expected to be valid in that neighborhood even though the flow is "slow" in the domain far from the walls. Flow visualization experiments by Sigli & Coutanceau (1977) for sphere *sedimentation* near finite boundaries in a tube to support this hypothesis since the viscoelastic effects were found to be large even though the nominal Weissenberg numbers were extremely small.

Acknowledgements—The authors thank Mr. William Fong for performing some of the experiments reported in this paper. This work was supported by a grant from the National Science Foundation. Experimental materials were generously donated by the Union Carbide Corp., B. F. Goodrich Co. and Dow Corning Co.

REFERENCES

- CHAN, P. C.-H. & LEAL, L. G. 1979 The motion of a deformable drop in a second-order fluid. *J. Fluid Mech.* **92**, 131.
- GOLDSMITH, H. L. & MASON, S. G. 1962 The flow of suspensions through tubes—I. Single spheres, rods and discs. *J. Colloid Sci.* **17**, 448.
- GAUTHIER, F., GOLDSMITH, H. L. & MASON, S. G. 1971a Particle motions in non-Newtonian media—II. Poiseuille flow. *Trans. Soc. Rheol.* **15**, 297.
- HO, B. P. & LEAL, L. G. 1976 Migration of rigid spheres in a two-dimensional unidirectional shear flow of a second-order fluid. *J. Fluid Mech.* **76**, 783.
- BRUNN, P. 1976a The slow motion of a sphere in a second-order fluid. *Rheol. Acta* **15**, 163.
- BRUNN, P. 1976b The behaviour of a sphere in non-homogeneous flows of a viscoelastic fluid. **15**, 589.
- KARNIS, A. & MASON, S. G. 1966 Particle motions in sheared suspensions—XIX. Viscoelastic media. *Trans. Soc. Rheol.* **10**, 571.
- GAUTHIER, F., GOLDSMITH, H. L. & MASON, S. G. 1971b Particle motions in non-Newtonian media—I. Couette flow. *Rheol. Acta* **10**, 344.
- KARNIS, A. & MASON, S. G. 1967 Particle motions in sheared suspensions—XXIII. Wall migration of fluid drops. *J. Colloid Interface Sci.* **24**, 164.
- TAYLOR, G. I. 1932 The viscosity of a fluid containing small drops of another fluid. *Proc. R. Soc. Lond.* **A138**, 41.
- KOVITZ, A. A. & YANNIMARAS, D. 1979 Interfacial tension measurements with a meniscal breakoff tensiometer. Presented at the 31st meeting of the Am. Phys. Soc., Div. of Fluid Dynamics.
- OLBRICHT, W. & LEAL, L. G. 1979 The motion of liquid drops through a converging-diverging tube of comparable diameter. Presented at the Golden Jubilee Meeting of the Soc. of Rheology.

- LEAL, L. G., SKOOG, J. & ACRIVOS, A. 1971 On the motion of gas bubbles in a viscoelastic liquid. *Can. J. Chem. Engng* **49**, 569.
- BLANKS, R. F., PARK, H. C., PATEL, D. R. & HAWLEY, M. C. 1974 A rheological study of aqueous Separan solutions. *Polymer Engng Sci.* **14**, 16.
- BEAVERS, G. S. & JOSEPH, D. D. (1975) The rotating rod viscometer. *J. Fluid Mech.* **69**, 475.
- GIESEKUS, H. 1966 Zur Stabilität von Strömungen viskoelastischer Flüssigkeiten—I. Ebene und kreisförmige Couette—Strömung. *Rheol. Acta* **5**, 239.
- LEAL, L. G. 1975 The slow motion of slender rod-like particles in a second-order fluid. **69**, 305.
- BARTRAM, E., GOLDSMITH, H. L. & MASON, S. G. 1975 Particle motions in non-Newtonian media—III. Further observations in elasticoviscous fluids. *Rheol. Acta* **14**, 776.
- GRACE, H. P. 1971 Dispersion phenomena in high viscosity immiscible fluid systems and application of static mixers and dispersion devices in such systems. DuPont Rep. An-15937.
- SIGLI, D. & COUTANCEAU, M. 1977 Effect of finite boundaries on the slow laminar isothermal flow of a viscoelastic fluid around a spherical obstacle. *J. Non-Newtonian Fluid Mech.* **2**, 1.